8-9-2007

Coupling Nanowire Chemiresistors with MEMS Microhotplate Gas Sensing Platforms

Douglas C. Meier
National Institute of Standards and Technology

Steve Semancik
National Institute of Standards and Technology

Bradley Button
Southern Illinois University Carbondale

Evgheni Strelcov
Southern Illinois University Carbondale

Andrei Kolmakov
Southern Illinois University Carbondale

Coupling nanowire chemiresistors with MEMS microhotplate gas sensing platforms

Douglas C. Meier and Steve Semancik
Chemical Science and Technology Laboratory, National Institute of Standards and Technology, Gaithersburg, Maryland 20899

Bradley Button, Evgheni Strelcov, and Andrei Kolmakov[a]
Department of Physics, Southern Illinois University, Carbondale, Illinois 62901

Recent advances in nanotechnology have yielded materials and structures that offer great potential for improving the sensitivity, selectivity, stability, and speed of next-generation chemical gas sensors. To fabricate practical devices, the "bottom-up" approach of producing nanoscale sensing elements must be integrated with the "top-down" methodology currently dominating microtechnology. In this letter, the authors illustrate this approach by coupling a single-crystal SnO_2 nanowire sensing element with a microhotplate gas sensor platform. The sensing results obtained using this prototype sensor demonstrate encouraging performance aspects including reduced operating temperature, reduced power consumption, good stability, and enhanced sensitivity. © 2007 American Institute of Physics. [DOI: 10.1063/1.2768861]

Chemical sensors have applications in many diverse sectors (e.g., environmental, automotive, medical, and homeland security). These applications require sensor technologies that are sensitive, selective, and broadly tunable. For general deployment, they must additionally be small, stable, robust, and cost effective. Miniaturized conductometric gas sensors developed at the National Institute of Standards and Technology (NIST) fulfill many of these requirements. While the development of fabrication technologies for microelectromechanical system (MEMS) devices have yielded a variety of small, low-powered sensors, further advances in materials development and integration are required before the benefits of nanostructured materials can be fully realized on these platforms.

Nanotechnology could provide sensing materials capable of improving the sensitivity, selectivity, stability, and speed of sensor technology. One recent area of interest involves applying quasi-one-dimensional (1D) metal oxide (MOX) nanostructures (nanowires, nanotubes, nanobelts, etc.) as prospective gas sensing elements.[1–5] The nanostructures' generically high surface area to bulk volume ratio and the comparability of their radii and their Debye lengths allows rapid transduction of surface interactions into measurable conductance changes. Fine control over the crystallinity, faceting, morphology, composition, and doping level of these structures has been demonstrated.[6–10] In addition, the 1D morphology of nanowires offers structurally and compositionally well-defined conducting channels on the micrometer scale, making them more easily integrable into existing microfabrication technology.[11,12]

Integrating quasi-1D nanomaterials with MEMS microhotplate platforms offers excellent prospects for advanced sensors. The μhp device (Fig. 1, top) consists of a micromachined suspended SiO_2 membrane featuring an embedded polycrystalline silicon heater and top contact Pt electrodes.[13] The sensing materials (e.g., MOX thin films,[14–16] nanoparticles,[17] microshells,[18] or conductive polymers[19]) are deposited on top of the electrodes. This device offers certain advantages: (i) due to the design, a single microchip can contain a large array of chemically and/or morphologically different sensing elements which can be operated independently; (ii) the low thermal inertia of this low-power sensor (approximately 22 mW is sufficient power to heat a single element to 500 °C) allows the implementation of thermal schedules, programmable on the order of milliseconds. These features are particularly useful when the microchip is used as an "electronic nose," since response orthogonality can be achieved for individual elements possessing unique temperature programs and material coatings due to variations in surface processes.[20,21]
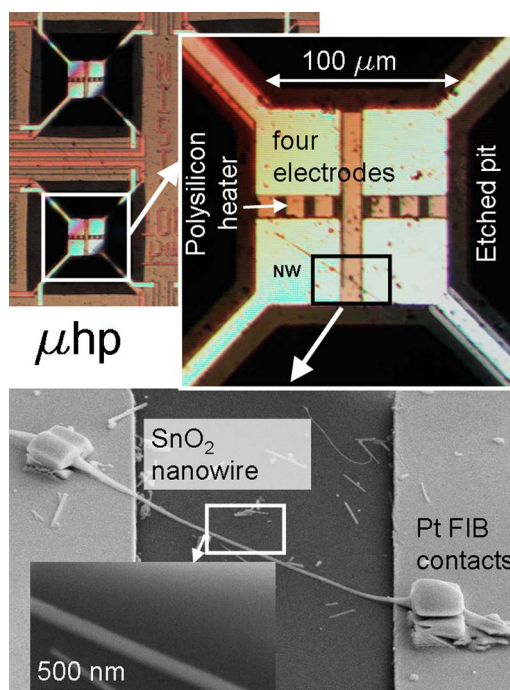

FIG. 1. (Color online) Top: optical image of a typical μhp architecture. Bottom: SEM image of the individual SnO_2 nanowire integrated as a chemiresistor using FIB technology.

[a]Electronic mail: akolmakov@physics.siu.edu

In this letter, we describe an advanced sensor device developed by integration of MOX nanowires with the μhp platform. The SnO_2 nanowires were synthesized using the vapor-solid growth method of flowing Ar (99.998%), carrier gas containing trace O_2 over a crucible of the source material, SnO. The product was collected from the 800 to 900 °C growth zones; its stoichiometry, morphology, and structure were studied using x-ray diffraction, scanning electron microscopy (SEM), and energy dispersive spectroscopy.[22] These studies confirmed the formation of rutile nanowire structures with an average diameter of approximately 100 nm. The individual nanowires were electrostatically picked up using a dielectric microfiber, then transferred to the μhps, and oriented to make contact with two of the contact pads. Square Pt patches (approximately $1 \times 1 \ \mu m^2$) were deposited using a focused ion beam SEM (FIB-SEM) to ensure that the electrical contacts were Ohmic. The sensors were cleaned with UV-O_3, then thermally activated by gradually heating (no faster than 14 °C/min) to 300 °C in zero-grade dry air for 30 min. This finished assembly functions as a "chemiresistor;" the conductance of the circuit completed by the nanowire is a function of its base conductance, its temperature, and the composition of the air with which it interacts. Under test conditions, the nanowire conductance was measured by applying a constant voltage across a circuit composed of the nanowire and a 1 ΩM series resistor, then comparing the voltage drop measured in each element of the circuit; the voltage drop across the nanowire was generally less than 1 V.

The typical sensing performance (the test apparatus is described in detail elsewhere[23]) of an individual nanowire sensor element when exposed to two reducing gases (NH_3 and CO) at concentrations of up to 100 μmol/mol (ppm) in dry air delivered at 1 standard L/min. is depicted in Fig. 2(a). As expected for the semiconducting nanowire, increasing temperature increases the baseline conductance exponentially. Similar to MOX thin film sensors, the response signals and response times [Fig. 2(a), insets] for these two target gases improves with increasing temperature, confirming the thermal activation of the redox reaction occurring at the nanowire surface. The maximum response ($\Delta G/G_0$) was achieved at approximately 260 °C [Fig. 2(b) circles]; measurable responses occur at as low as 100 °C. The response time constant decreases as the sensor temperature increases [Fig. 2(b), squares], a consequence of the temperature-dependent interaction of the analyte with the oxide depletion layer.

The nanowire sensor sensitivity to NH_3 is approximately ten times greater than it is to CO. Such selectivity is a result of the lower efficiency of surface charge transfer during the CO oxidation reaction, as was observed previously for SnO_2 thin films and nanostructures.[24] Transduction mechanisms have been extensively elaborated in the literature.[25] As previously observed, the small thermal inertia of the μhp allows not only prompt determination of the optimal temperature regime [Fig. 2(b)], but also makes possible the implementation of predesigned rapid temperature excursions to enhance selectivity. During these temperature-programed sensing (TPS) measurements,[21] the conductance response of the sensor is measured as a function of the programed temperature. Since the signal arising from adsorption/desorption, redox, and decomposition processes for any given analyte-sensor material pair are temperature dependent, such ramps can pro-
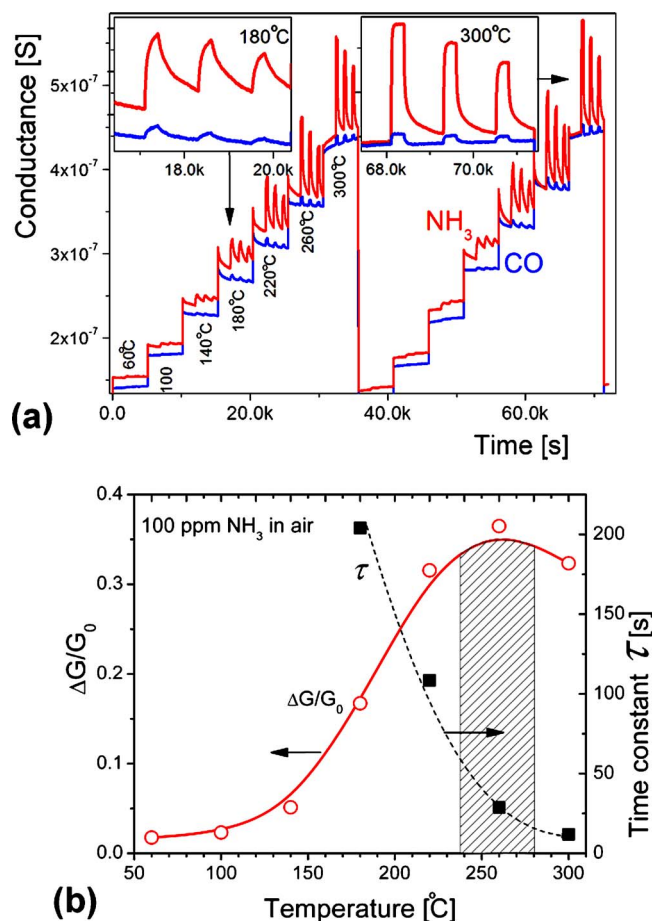

FIG. 2. (Color online) (a) Sensor responses to NH_3 (top curve, red) and CO (bottom curve, blue) at 100, 50, and 25 ppm sequential pulses in dry air measured at a series of temperatures from 60 to 300 °C. The curves have the same background conductance but have been offset for clarity. A second excursion through the temperature cycle was completed to confirm signal repeatability. The inserts are "zoomed" isothermal regions to show the increase of the signal onset rates with temperature. (b) The temperature dependence of the sensor response to 100 ppm of NH_3 (red circles). Included (black squares) is the corresponding temperature dependence of the signal onset time constant. The optimal performance is achieved in the shaded region.

vide "fingerprints" for analyte identification. The feasibility of TPS for measuring CO using a SnO_2 nanowire sensor is depicted in Fig. 3. The TPS response to 100 ppm of CO compared to background dry air shows a signal level increase and a shift of the signature's maximum to lower temperature. The repeatability of this analyte signature is apparent.

A further examination of the sensitivity and dynamic detection range of this nanowire sensor prototype was performed using NH_3 as the analyte (Fig. 4). The signal-to-noise ratio allows the detection of as low as 30 nmol/mol [(ppb) defined as parts per 10^9] of NH_3 in air. The conductance response $\Delta G = G_{gas} - G_{air}$ follows a power law relationship with the analyte concentration C: $\Delta G \approx C^{\alpha}$, with the exponent very close to 0.5 (Fig. 4, inset). This relation holds through an analyte concentration excursion spanning four orders of magnitude. According to a model developed previously,[25] three conclusions are implied: (i) that the approximation of the completely depletable conduction channel $R \approx \lambda_D$ (where R is the radius of the nanowire and λ_D the Debye length of the material at the given temperature) can be applied to the nanowire, (ii) that singly charged O^- is the
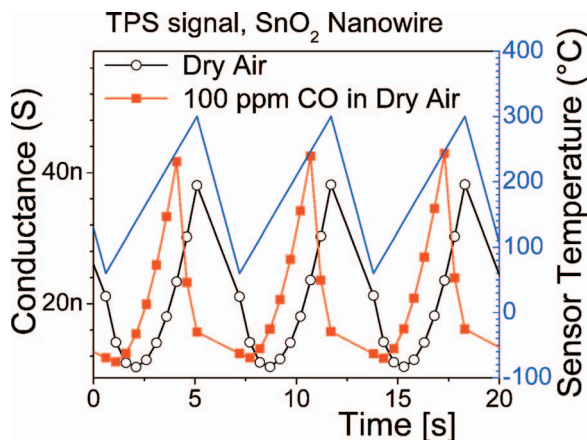
FIG. 3. (Color) Temperature-programed sensing (TPS) measurements, where the blue triangular wave (top) is the temperature profile of the sensor in time, and the black circles and red squares show the nanowire conductance measurements upon exposure to dry air and 100 ppm CO, respectively. The distinct differences between the signal patterns can serve as a means of discrimination.

predominant ionosorbed species that reacts with reducing gases, and (iii) since signal saturation did not occur, $\theta(NH_3) \ll \theta(O^-)$ in the tested analyte concentration range. Furthermore, since the nanowire is a single-crystal conducting channel, the model can be readily applied, as opposed to the situation for conventional MOX nanoparticle films, where lesser-defined percolation between multiple nanocrystalline grains complicates the signal analysis.

In conclusion, the coupling of single-crystal nanowire sensing elements with μhp sensing platforms demonstrates a prospective method of fabricating future chemical sensors with advanced sensitivity, stability, speed, and (potentially) selectivity. Due to the well-defined composition, crystallinity, and morphology of the sensing element, the performance of such conductometric sensors can be modeled more simply
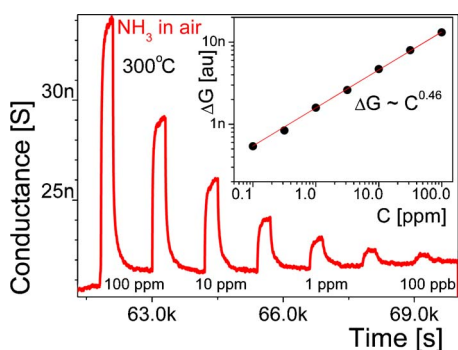

FIG. 4. (Color online) Conductance response to NH$_3$ pulses in air (100 ppm−100 nmol/mol (ppb) step √10/10 power law) measured at 300 °C. In the inset, the conductance increase as a function of NH$_3$ concentration is shown (log-log scale). The solid line shows the data fit with a power law curve.

than polycrystalline devices (i.e., conventional sensing films), which is a considerable advantage compared to the phenomenological approach currently used to describe thin/thick film MOX sensors.

[1] A. Kolmakov and M. Moskovits, Annu. Rev. Mater. Res. **34**, 151 (2004).
[2] E. Comini, Anal. Chim. Acta **568**, 28 (2006).
[3] J. G. Lu, P. C. Chang, and Z. Y. Fan, Mater. Sci. Eng., R. **52**, 49 (2006).
[4] A. Kolmakov, Int. J. Nanotechnol. (to be published).
[5] Z. L. Wang, Annu. Rev. Phys. Chem. **55**, 159 (2004).
[6] L. J. Lauhon, M. S. Gudiksen, and C. M. Lieber, Philos. Trans. R. Soc. London, Ser. A **362**, 1247 (2004).
[7] S. Dmitriev, Y. Lilach, B. Button, M. Moskovits, and A. Kolmakov, Nanotechnology **18**, 055707 (2007).
[8] S. J. Pearton, D. P. Norton, Y. W. Heo, L. C. Tien, M. P. Ivill, Y. Li, B. S. Kang, F. Ren, J. Kelly, and A. F. Hebard, J. Electron. Mater. **35**, 862 (2006).
[9] C. Li, D. H. Zhang, B. Lei, S. Han, X. L. Liu, and C. W. Zhou, J. Phys. Chem. B **107**, 12451 (2003).
[10] A. Kolmakov, Proc. SPIE **6370**, 63700X-5 (2006).
[11] C. Yu, Q. Hao, S. Saha, L. Shi, X. Y. Kong, and Z. L. Wang, Appl. Phys. Lett. **86**, 063101 (2005).
[12] F. Patolsky, G. Zheng, and C. M. Lieber, Nanomedicine **1**, 51 (2006).
[13] S. Semancik, R. E. Cavicchi, M. Gaitan, and J. S. Suehle, US Patent No. 5,345,213 (6 September 1994).
[14] R. E. Cavicchi, S. Semancik, F. DiMeo, and C. J. J. Taylor, J. Electroceram. **9**, 155 (2003).
[15] S. Semancik, R. E. Cavicchi, K. G. Kreider, J. S. Suehle, and P. Chaparala, Sens. Actuators B **34**, 209 (1996).
[16] B. Panchapakesan, D. L. Devoe, M. R. Widmaier, R. Cavicchi, and S. Semancik, Nanotechnology **12**, 336 (2001).
[17] K. D. Benkstein and S. Semancik, Sens. Actuators B **113**, 445 (2006).
[18] C. J. Martinez, B. Hockey, C. B. Montgomery, and S. Semancik, Langmuir **21**, 7937 (2005).
[19] G. F. Li, C. Martinez, J. Janata, J. A. Smith, M. Josowicz, and S. Semancik, Electrochem. Solid-State Lett. **7**, H44 (2004).
[20] Z. Boger, D. C. Meier, R. E. Cavicchi, and S. Semancik, Sens. Lett. **1**, 86 (2003).
[21] T. A. Kunt, T. J. McAvoy, R. E. Cavicchi, and S. Semancik, Sens. Actuators B **53**, 24 (1998).
[22] V. V. Sysoev, B. K. Button, K. Wepsiec, S. Dmitriev, and A. Kolmakov, Nano Lett. **6**, 1584 (2006).
[23] M. C. Wheeler, J. E. Tiffany, R. M. Walton, R. E. Cavicchi, and S. Semancik, Sens. Actuators B **77**, 167 (2001).
[24] C. Baratto, E. Comini, G. Faglia, G. Sberveglieri, M. Zha, and A. Zappettini, Sens. Actuators B **109**, 2 (2005).
[25] N. Barsan and U. Weimar, J. Electroceram. **7**, 143 (2001).